

# INTERACTIONS OF $K^-$ MESONS IN HYDROGEN IN THE 300 TO 850 MeV/c REGION (\*)

**P. L. Bastien, J. P. Berge, O. I. Dahl, M. Ferro-Luzzi, J. Kirz, D. H. Miller, J. J. Murray, A. H. Rosenfeld, R. D. Tripp and B. Watson**

Lawrence Radiation Laboratory and Department of Physics, University of California, Berkeley, Cal.

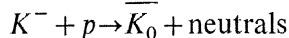
(presented by A. H. Rosenfeld)

Results are presented on the total and partial cross-sections for  $K^-$  mesons incident on protons at laboratory momenta of 293, 350, 390, 434, 513, 620, 762, and 850 MeV/c. We have studied the interactions in the Lawrence Radiation Laboratory's 15" hydrogen bubble chamber, using a purified  $K^-$  beam. For each momentum setting, a total of several thousand interactions has been recorded and analyzed.

The value of the path length was obtained at each momentum from the number of  $\tau$ -decays; the scanning efficiency for these events (of the order of 95%) is much higher than that for the more frequent one-prong decays. This compensates for the reduction in statistics.

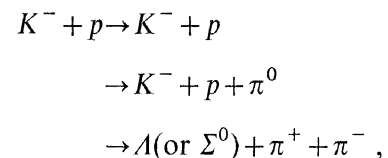
As they appear in the bubble chamber, the interactions fall naturally into one of the following categories (only those reactions kinematically allowed at our momenta are listed):

(a) **Zero prongs.** These are due to the reactions



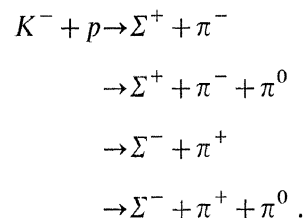
where the  $K^0$  and the  $\Lambda$  decay via the neutral mode or escape from the chamber. However, the pion contamination in the beam (of the order of 10 to 30%) adds  $\pi^-$  charge-exchange reactions to this class; hence no measurements are practical. Instead the contribution of these reactions to the cross-section are accounted for by using the known neutral-to-charged decay branching ratios of the  $\overline{K}^0$  and  $\Lambda$ , and the "zero-prong+ $V$ " data [see (e) below].

(b) **Two-prongs.** These are due to



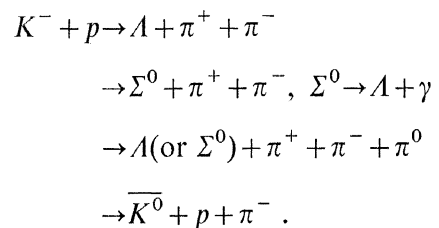
where the  $\Lambda$  decays via its neutral mode or escapes observation [see (d) for the  $\Lambda$ -charged-mode counterpart of this case]. Reactions producing a very short  $\Sigma$  may also appear as a two-prong event. Analysis of the events by the PANG and KICK computer programs allows separation of the above reactions.

(c)  **$\Sigma$ -one-prong.** These are due to



The computer programs easily separate the elastic from the inelastic processes.

(d) **Two-prong+ $V$ .** These are due to charged-mode decays of  $\Lambda$  and  $\overline{K}^0$  from



(\*) Work done under the auspices of the U.S. Atomic Energy Commission.

Separation of the reactions is accomplished by the kinematical programs plus ionization estimates in case of ambiguities. To compute cross-sections for the above reactions, one multiplies the number of events with a  $\Lambda$  by 3/2 and those with a  $\bar{K}^0$  by 3.

(e) **Zero-prong+V.** These are due to charged-mode decays of  $\Lambda$  and  $\bar{K}^0$  from

$$\begin{aligned}
 K^- + p &\rightarrow \Lambda + \pi^0, \\
 &\rightarrow \Lambda + \pi^0 + \pi^0, \\
 &\rightarrow \Lambda + \pi^0 + \pi^0 + \pi^0, \\
 &\rightarrow \Sigma^0 + \pi^0, \quad \Sigma^0 \rightarrow \Lambda + \gamma, \\
 &\rightarrow \Sigma^0 + \pi^0 + \pi^0, \\
 &\rightarrow \bar{K}^0 + n, \\
 &\rightarrow \bar{K}^0 + n + \pi^0.
 \end{aligned}$$

In this case the separation is based on the decay fit for the  $V$ .  $\Lambda$  and  $\bar{K}^0$  decays are distinguished (ambiguities being resolved by ionization); then we compute the total mass recoiling against the  $\Lambda$  or the  $\bar{K}^0$  in the  $K^-p$  centre-of-mass. From the shape of the mass spectrum, a subdivision is further possible into the various channels. In order to account for the

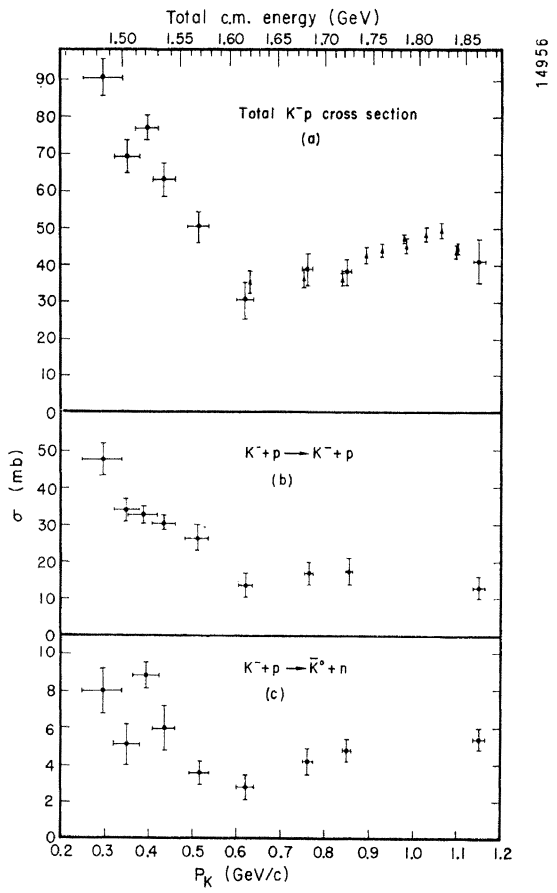


Fig. 1 (a) Total  $K^-p$  cross-section. The triangles represent the results of the counter experiments of reference 2. The point at 1.15 GeV/c comes from reference 1. (b)  $K^-+p \rightarrow K^-+p$  cross-section. (c)  $K^-+p \rightarrow \bar{K}^0+n$  cross-section.

TABLE I

Values of the cross-sections in mb for  $K^-+p$  reactions as a function of the  $K^-$  laboratory momentum

| $P_K$ (MeV/c) =                    | 293 $\pm$ 42    | 350 $\pm$ 31    | 390 $\pm$ 30    | 434 $\pm$ 26    | 513 $\pm$ 20    | 620 $\pm$ 15    | 762 $\pm$ 8     | 850 $\pm$ 10    |
|------------------------------------|-----------------|-----------------|-----------------|-----------------|-----------------|-----------------|-----------------|-----------------|
| CM Energy (Mev)                    | 1480            | 1500            | 1520            | 1555            | 1570            | 1620            | 1680            | 1720            |
| $K^-p$                             | 48.2 $\pm$ 4.2  | 34.0 $\pm$ 3.2  | 32.7 $\pm$ 1.8  | 30.6 $\pm$ 3.4  | 26.5 $\pm$ 3.3  | 13.8 $\pm$ 3.0  | 17 $\pm$ 3      | 17.5 $\pm$ 4    |
| $\bar{K}^0n$                       | 8.0 $\pm$ 1.2   | 5.1 $\pm$ 1.1   | 8.8 $\pm$ 0.7   | 6.0 $\pm$ 1.2   | 3.6 $\pm$ 0.6   | 2.8 $\pm$ 0.7   | 4.2 $\pm$ 0.7   | 4.8 $\pm$ 0.6   |
| $\Sigma^+\pi^-$                    | 13.6 $\pm$ 1.4  | 10.6 $\pm$ 1.4  | 12.5 $\pm$ 0.08 | 8.2 $\pm$ 0.9   | 7.5 $\pm$ 1.1   | 4.5 $\pm$ 0.5   | 3.0 $\pm$ 0.2   | 2.0 $\pm$ 0.2   |
| $\Sigma^-\pi^+$                    | 10.0 $\pm$ 1.1  | 6.9 $\pm$ 1.0   | 6.9 $\pm$ 0.5   | 6.1 $\pm$ 0.7   | 4.9 $\pm$ 0.8   | 2.1 $\pm$ 0.4   | 3.3 $\pm$ 0.3   | 1.6 $\pm$ 0.2   |
| $\Sigma^0\pi^0$                    | 5.2 $\pm$ 0.9   | 6.3 $\pm$ 1.4   | 6.7 $\pm$ 0.6   | 4.9 $\pm$ 1.3   | 1.7 $\pm$ 0.3   | 2.3 $\pm$ 0.5   | 1.8 $\pm$ 0.4   | 0.9 $\pm$ 0.3   |
| $\Lambda\pi^0$                     | 5.2 $\pm$ 0.9   | 4.5 $\pm$ 1.0   | 3.1 $\pm$ 0.3   | 3.2 $\pm$ 0.7   | 1.6 $\pm$ 0.4   | 2.6 $\pm$ 0.5   | 2.2 $\pm$ 0.4   | 2.8 $\pm$ 0.5   |
| $\Lambda(\Sigma^0)\pi^0\pi^0$      | 0.3 $\pm$ 0.2   | 1.9 $\pm$ 0.6   | 1.5 $\pm$ 0.2   | 0.8 $\pm$ 0.4   | 1.1 $\pm$ 0.3   | 0.8 $\pm$ 0.2   | 2.0 $\pm$ 0.4   | 1.4 $\pm$ 0.3   |
| $\Lambda\pi^+\pi^-$                | 0.15 $\pm$ 0.1  | 0.9 $\pm$ 0.3   | 1.6 $\pm$ 0.2   | 1.5 $\pm$ 0.4   | 2.0 $\pm$ 0.4   | 1.8 $\pm$ 0.3   | 3.3 $\pm$ 0.3   | 3.2 $\pm$ 0.3   |
| $\Lambda(\Sigma^0)\pi^+\pi^-\pi^0$ | —               | —               | —               | —               | 0 $\pm$ 0.01    | 0 $\pm$ 0.03    | 0.25 $\pm$ 0.05 | 0.15 $\pm$ 0.05 |
| $\Sigma^+\pi^-\pi^0$               | 0 $\pm$ 0.05    | 0.06 $\pm$ 0.06 | 0.11 $\pm$ 0.04 | 0.18 $\pm$ 0.11 | 0.2 $\pm$ 0.12  | 0.2 $\pm$ 0.13  | 0.7 $\pm$ 0.1   | 0.6 $\pm$ 0.1   |
| $\Sigma^-\pi^+\pi^0$               | 0.05 $\pm$ 0.05 | 0 $\pm$ 0.06    | 0.12 $\pm$ 0.05 | 0 $\pm$ 0.06    | 0.14 $\pm$ 0.10 | 0.4 $\pm$ 0.15  | 0.8 $\pm$ 0.1   | 0.7 $\pm$ 0.1   |
| $\Sigma^0\pi^+\pi^-$               | 0 $\pm$ 0.02    | 0 $\pm$ 0.09    | 0.07 $\pm$ 0.06 | 0 $\pm$ 0.08    | 0.3 $\pm$ 0.15  | 0.3 $\pm$ 0.1   | 0.7 $\pm$ 0.1   | 0.8 $\pm$ 0.1   |
| $\bar{K}^0p\pi^-$                  | —               | —               | —               | —               | —               | 0 $\pm$ 0.03    | 0.04 $\pm$ 0.03 | 0.10 $\pm$ 0.06 |
| $K^-p\pi^0$                        | —               | —               | —               | —               | —               | 0.06 $\pm$ 0.06 | 0.13 $\pm$ 0.1  | 1.0 $\pm$ 0.4   |
| $K^-\pi^+n$                        | —               | —               | —               | —               | —               | 0.06 $\pm$ 0.06 | 0 $\pm$ 0.1     | 0.2 $\pm$ 0.1   |
| Total                              | 90.7 $\pm$ 4.9  | 70.2 $\pm$ 4.2  | 73.8 $\pm$ 2.3  | 61.5 $\pm$ 4.1  | 49.5 $\pm$ 3.7  | 30.3 $\pm$ 5.0  | 38.2 $\pm$ 4.0  | 37.3 $\pm$ 4.0  |

loss of those events without a visible decay, here as in (d) one multiplies by 3/2 for the  $\Lambda$ 's and by 3 for the  $\bar{K}^0$ 's before computing cross-sections.

The values obtained for the cross-sections are collected in Table I and are also shown in Fig. 1-3. All values at  $P_K = 1.15$  GeV/c come from reference 1. Also shown are the total cross-sections obtained in counters experiments <sup>2)</sup>.

Inspection of the graphs leads to the following observations:

1. In the low-momentum region, the presence of the excited hyperon  $Y_0^*$  (1520) is manifest from the enhancements occurring for the various channels around  $P_K = 400$  MeV/c <sup>3)</sup>.
2. A sudden increase in  $\Lambda\pi^+\pi^-$  production occurs at about 760 MeV/c, corresponding to copious production of the excited hyperon  $Y_1^*$  (1385) via the reaction  $K^- + p \rightarrow Y_1^{*\pm} \pi^\mp$  <sup>4)</sup>.

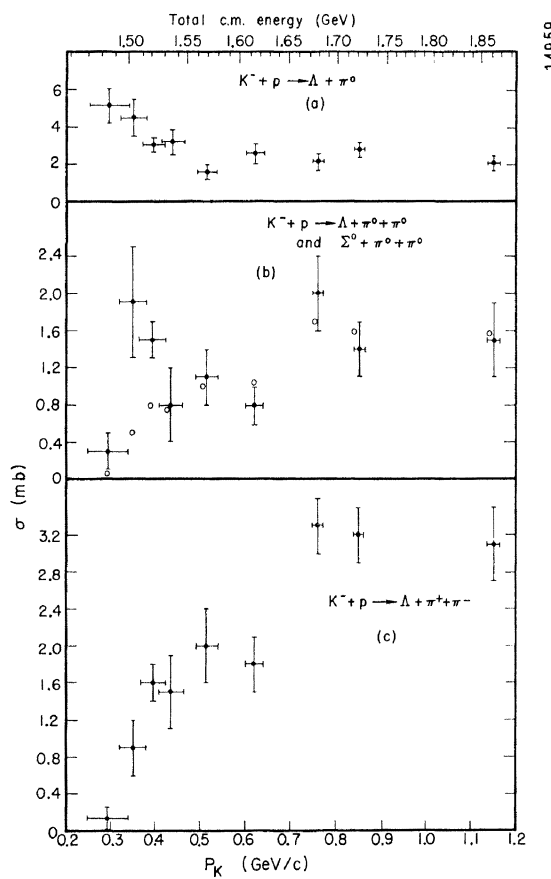


Fig. 2 Cross-sections for the reactions (a)  $K^- + p \rightarrow \Lambda + \pi^0$ , (b)  $K^- + p \rightarrow \Lambda$  (or  $\Sigma^0$ )  $\pi^0 + \pi^0$ , and (c)  $K^- + p \rightarrow \Lambda + \pi^+ + \pi^-$ . Cross-section (b) includes production of  $\eta_{\text{neutral}}$  (only the neutral decay mode of  $\eta$  falls into this category). At 760 MeV/c,  $\sigma(\Lambda + \eta_{\text{neutral}})$  is estimated to be  $0.48 \pm 0.10$  mb; at 850 MeV/c,  $\sigma$  is less than  $0.02 \pm 0.02$  mb. The open circles represent upper limits from charge independence ( $\sigma_{\Lambda\pi^0\pi^0} \leq \sigma_{\Lambda\pi^+\pi^-}/2$ ). Cross-section (c) includes  $Y_1^*$  (1385) +  $\pi$  production; at 760 MeV/c,  $\sigma(Y_1^{*\pm} + \pi) = 2.4 \pm 0.3$  mb, at 850 MeV/c,  $\sigma(Y_1^{*\pm} + \pi) = 1.9 \pm 0.5$  mb.

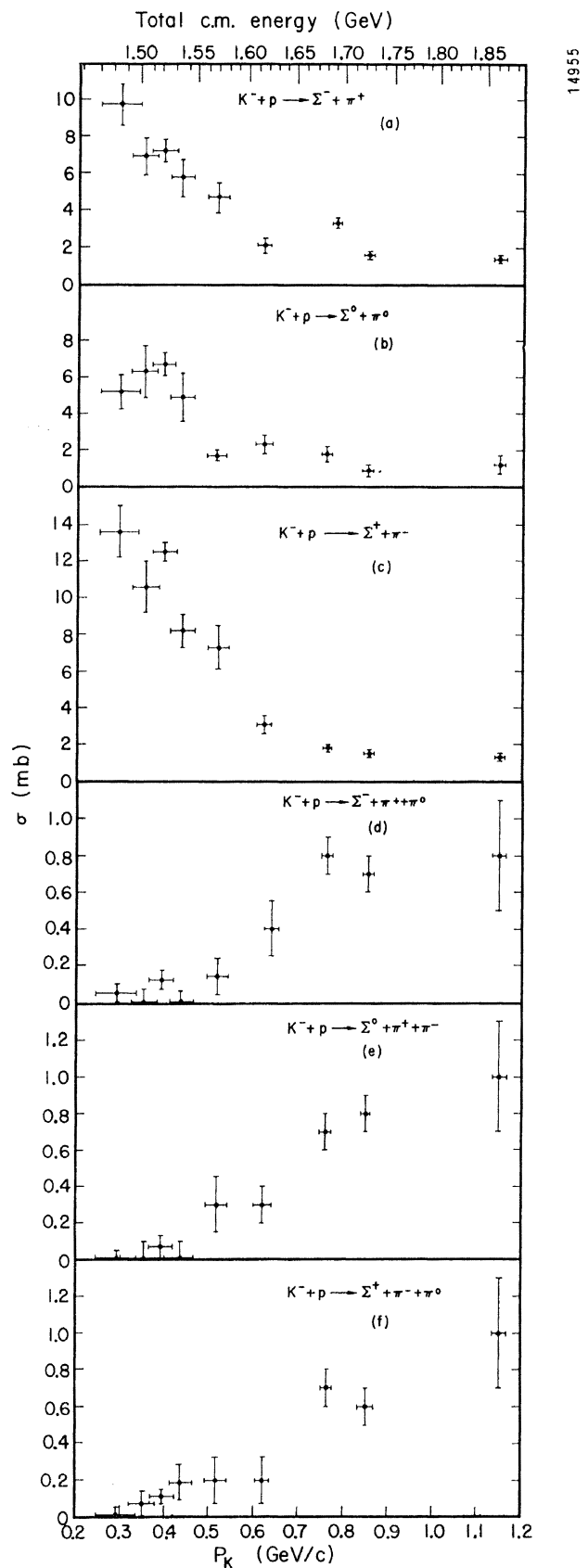


Fig. 3 Cross-sections for the reactions (a)  $K^- + p \rightarrow \Sigma^- + \pi^+$ , (b)  $K^- + p \rightarrow \Sigma^0 + \pi^0$ , (c)  $K^- + p \rightarrow \Sigma^+ + \pi^-$ , (d)  $K^- + p \rightarrow \Sigma^- + \pi^+ + \pi^0$ , (e)  $K^- + p \rightarrow \Sigma^0 + \pi^+ + \pi^-$ , and (f)  $K^- + p \rightarrow \Sigma^+ + \pi^- + \pi^0$ .

3. Some enhancement in the  $\Sigma\pi$  channels, mainly  $\Sigma^-\pi^+$ , is apparent at about 760 MeV/c, corresponding to a total c.m. energy of about 1680 MeV. This observation, together with strong indications of a sudden change in the differential cross-sections for the  $\Sigma\pi$  reactions at this momentum, suggests the

possible existence of a new excited hyperon with total mass  $\sim 1680$  MeV<sup>5)</sup>.

Further details on the analysis and a study of the differential cross-sections will be presented in later publications.

#### LIST OF REFERENCES

1. W. Graziano and S. G. Wojcicki,  $K^-p$  Interactions at 1.15 BeV/c., Lawrence Radiation Laboratory Report UCRL-10177, April 17, 1962 (unpublished).
2. V. Cook, B. B. Cork, T. F. Hoang, D. Keefe, L. T. Kerth, W. A. Wenzel, and T. F. Zipf, Phys. Rev. 123, 320 (1961); O. Chamberlain, K. M. Crowe, D. Keefe, L. T. Kerth, A. Lemonick, Tin Maung, and T. F. Zipf, Phys. Rev. 125, 1696 (1962).
3. M. Ferro-Luzzi, R. D. Tripp and M. B. Watson, Phys. Rev. Letters, 8, 28 (1962); R. D. Tripp, M. B. Watson, and M. Ferro-Luzzi, Phys. Rev. Letters, 8, 175 (1962).
4. M. H. Alston and M. Ferro-Luzzi, Revs. Modern Phys. 33, 416 (1961).
5. Indications for the existence of such a 1680-MeV  $\Sigma\pi$  resonance have also been observed in  $\pi-p$  data by G. Alexander, L. Jacobs, G. R. Kalbfleisch, D. H. Miller, G. A. Smith, and J. A. Schwartz. (See p. 320).

## **$K^-p$ CHARGE EXCHANGE AT 1.22 GeV/c<sup>(\*)</sup>**

**M. Ferro-Luzzi, F. T. Solmitz and M. L. Stevenson**

Lawrence Radiation Laboratory, University of California, Berkeley, Cal.

(presented by A. H. Rosenfeld)

The reaction



has been studied at an incident  $K^-$  momentum of 1.22 GeV/c (1895 MeV total c.m. energy) using the L.R.L. 72" hydrogen bubble chamber and a separated  $K^-$  beam. The angular distribution for the reaction in the centre-of-mass shows a prominent backward peaking of the  $\bar{K}^0$ . This behaviour had been noticed in earlier experiments at lower  $K^-$  incident momenta, starting at about 760 MeV/c<sup>1)</sup> and growing steadily up to the present momentum. Preliminary results at 1.53 GeV/c incident momentum (2025 MeV total

c.m. energy) indicate the effect to have disappeared or, at any rate, to have lost its spectacular character.

The events appear in the chamber as incident tracks which interact in flight without outgoing charged prongs, accompanied by the two-prong decay of a neutral particle. The measurement of the associated decay products usually suffices to identify the decaying particle as  $K^0$  or  $\Lambda$ . Cases of ambiguous kinematical fit are solved in general by ionization estimates on the positive track; a  $\chi^2$  criterion was imposed on the decay configuration such that only  $\sim 1\%$  of a pure sample of  $K_1^0 \rightarrow \pi^+ + \pi^-$  would fail to satisfy it.

(\*) Work done under the auspices of the U.S. Atomic Energy Commission.